

Supplementary Information

Microfluidic solvent extraction of poly (vinyl alcohol) droplets: effect of polymer structure on particle and capsule formation

W. N. Sharratt,^a A. Brooker,^b E. S. J. Robles,^b and J. T. Cabral^{a*}

^a Department of Chemical Engineering, Imperial College London, London SW7 2AZ, United Kingdom.
Email: j.cabral@imperial.ac.uk

^b Procter & Gamble, Newcastle Innovation Centre, Newcastle-Upon-Tyne NE12 9TS, United Kingdom

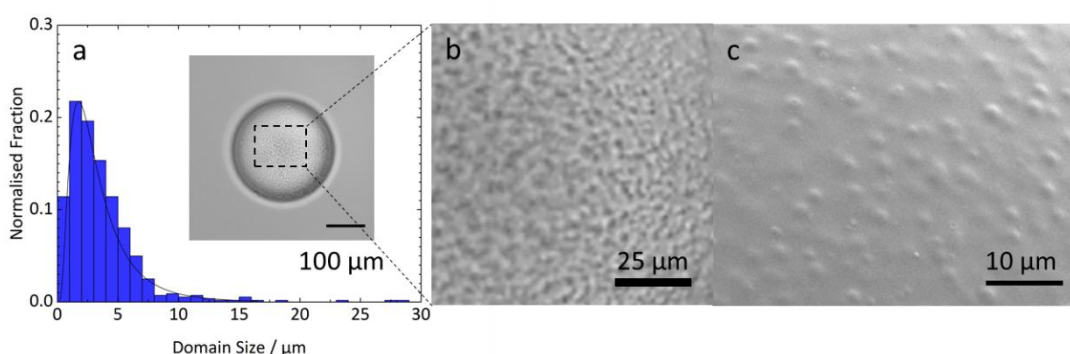


Figure S1: (a) Histogram for domain size of the phase separated structure shown Figure 2. The size of phase separated domains, referred to in the main text as characteristic length, was approximately several μm . A log-normal distribution is fitted to guide the eye. (Inset) Brightfield image of a typical polymer solution droplet undergoing demixing during the solvent extraction process. (b) Enlarged area of the demarcated area in the inset of (a) where the phase separated structure is most visible. (c) Magnified (1400X) scanning electron micrograph of a dried particle surface subsection. The surface was covered with small dimples with sizes of a similar magnitude to the demixed domains during the extraction process.

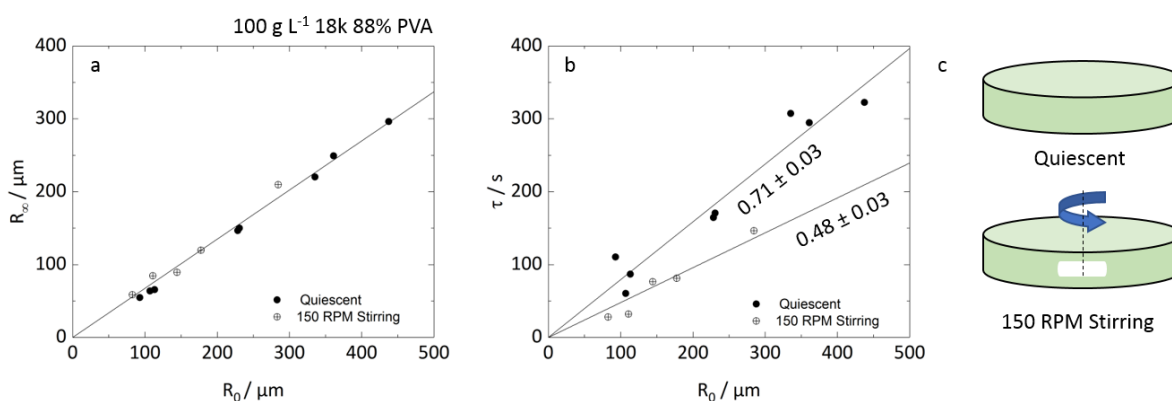


Figure S2: Comparison between droplet extraction (100 g L⁻¹ 18k 88% PVA) in the absence and presence of external flow (illustrated by stirring at 150 rpm approximately 3 cm away from the droplet). (a) The dependence of the final particle size, R_∞ , on the initial droplet size, R_0 , appears unchanged, while (b) extraction timescale, τ , decreases in all cases approximately 40% with stirring. Schematics of the setup are provided in (c). The timescales for H₂O diffusion within EA extraction medium can be estimated to be on the order of 10 s (3-50 s) for distances $\approx R_0$ investigated (based on diffusion coefficients reported in [1]). Since these timescales are commensurate with τ , it is thus expected that additional convection (imposed by stirring) will expedite H₂O removal from the vicinity of the droplet and thus decrease τ .

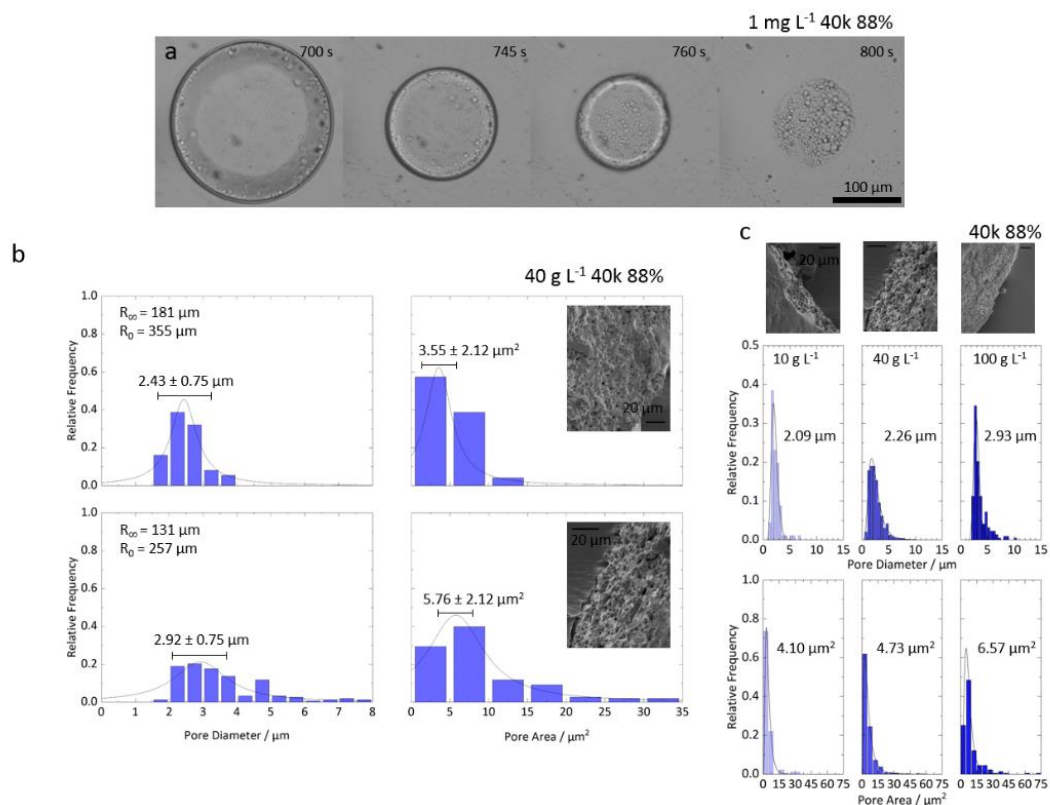


Figure S3: (a) Bright field optical microscopy images during a narrow time window of extraction of a 1 mg L^{-1} 40k 88% PVA solution droplet showing some degree of coarsening of the internal demixed structure. For this system, the effect is, however, modest, varying by an order of one μm or so until kinetic arrest. (b) Internal pore diameters and areas, extracted from SEM images (shown in inset) for two particles of different initial droplet size (R_0), showing a small variation, within measurement uncertainty. (c) Effect of initial polymer concentration on the pore diameter and area for 40k 88% PVA polymer particles, showing that these are nearly identical, within measurement uncertainty ($\pm 0.8 \mu\text{m}$ and $\pm 2 \mu\text{m}^2$ for pore diameter and pore area respectively). The insensitivity of the PVA/water system contrasts with the significant coarsening observed in other systems (e.g. NaPSS/water [2-4]), and is discussed in the main text.

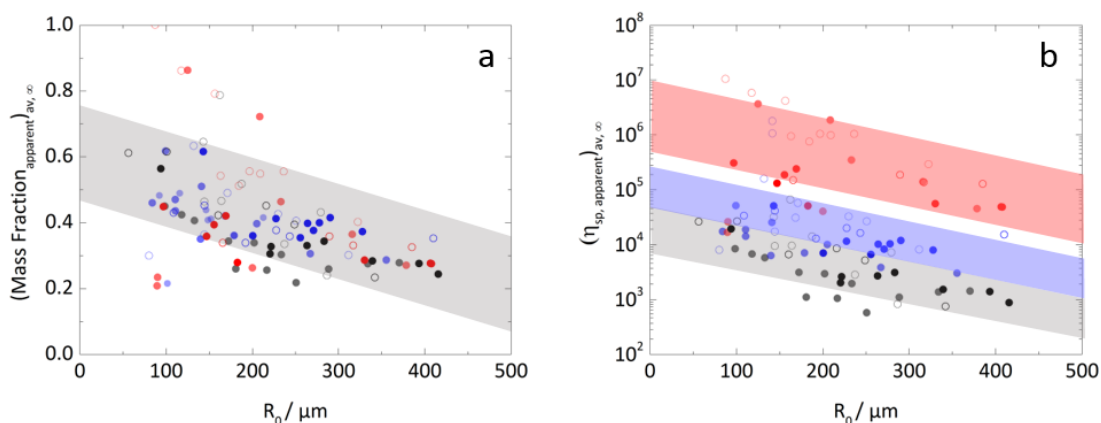


Figure S4: (a) Final average polymer concentration in microparticles, estimated over the particle volume and calculated by mass conservation, for various initial droplet sizes (R_0). Light coloured markers represent 40 g L^{-1} initial polymer concentration of droplets whilst full colour markers represent 100 g L^{-1} . A broad band is indicated to illustrate the trend with R_0 for the apparent concentration and the lack of difference, within experimental uncertainty, of M_w , initial concentration (above c^*) and degree of hydrolysis. (b) Average specific viscosity calculated from the concentration data in (a) as a function of R_0 . Due to the scaling of viscosity with M_w , the similar average apparent mass content within the polymer particles upon solidification stratify into discrete bands for each molecular weight (combined concentration and degree of hydrolysis).

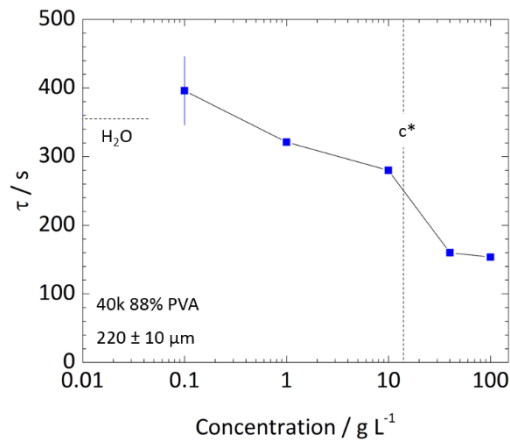


Figure S5: Concentration dependence of the extraction time, τ , for polymer solution droplets of 40k 88% PVA and constant $R_0 = 220 \pm 10 \mu\text{m}$. The extraction time for pure water is indicated by the horizontal dashed line. Above c^* the extraction time was found to remain approximately constant, within experimental uncertainty.

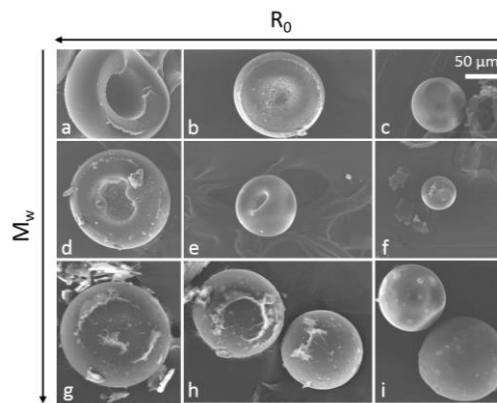


Figure S6: SEM images of the microparticle formed by solvent extraction of 40 g L^{-1} PVA solutions of varying molecular weight and initial droplet size (R_0). The images mainly focus on the microparticle side in contact with partially wetting substrate during the ex-situ extraction process. The morphology of particle became more indented, on that side, with increasing R_0 and decreasing molecular weight. Conversely, particles templated from a higher molecular weight polymer at the same initial concentration, and from smaller R_0 , formed more compact and less deformed particles. (A-C): 18k 88%. (D-F): 40k 99%. (G-I): 105k 88%.

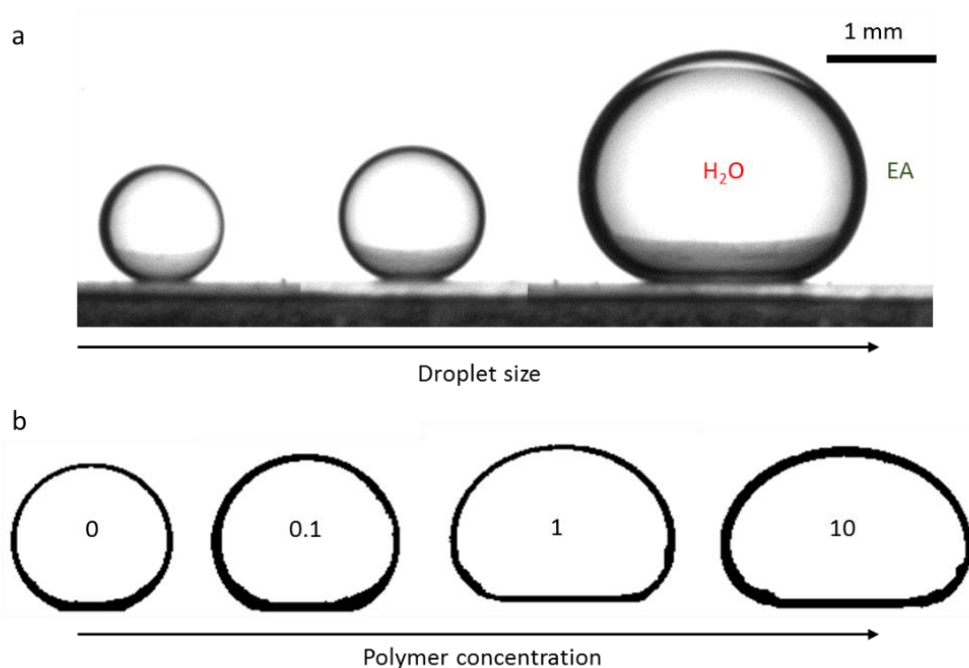


Figure S7: (a) Variation of droplet morphology for pure water on an OTS treated substrate for increasing droplet sizes. The capillary length for aqueous droplets of PVA was calculated to reside between 722-832 μm (dependent on concentration and assuming solution density is bounded by the density of pure H₂O and pure PVA). As can be seen, the deformation due to gravity and contact diameter (the area in contact with the substrate) increased as droplet size increased. (b) Image contours for polymer solution droplets, of equivalent volume ($\sim 1 \mu\text{L}$), as a function of polymer concentration. Numbers correspond to the % w/w of the 40k 88% PVA solution used. Contact diameter and deformation due to gravity increased with increasing polymer concentration. All droplets had characteristic lengths (radii) greater than that of their corresponding capillary length i.e. > 722 or $832 \mu\text{m}$.

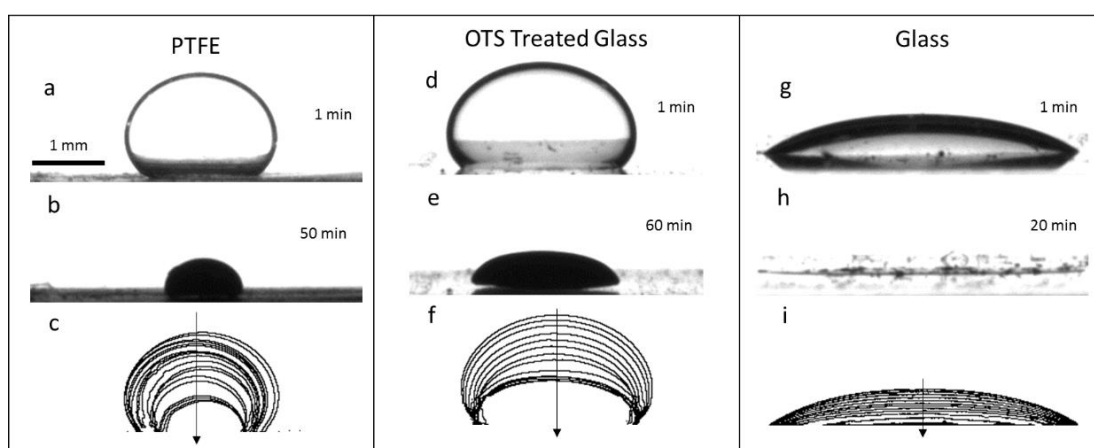


Figure S8: Effect of substrate on droplet extraction. Images were acquired in two-minute intervals following immersion of droplets into non-solvent. The sample chamber was mounted on a Rame-Hart goniometer with tiltable stage, camera and uniform illumination source. Initial (a, d, g) and final (b, e, h) images are shown alongside droplet contours for the temporally-resolved process (c, f, i). Droplet volume was $\sim 1 \mu\text{L}$ in all cases.

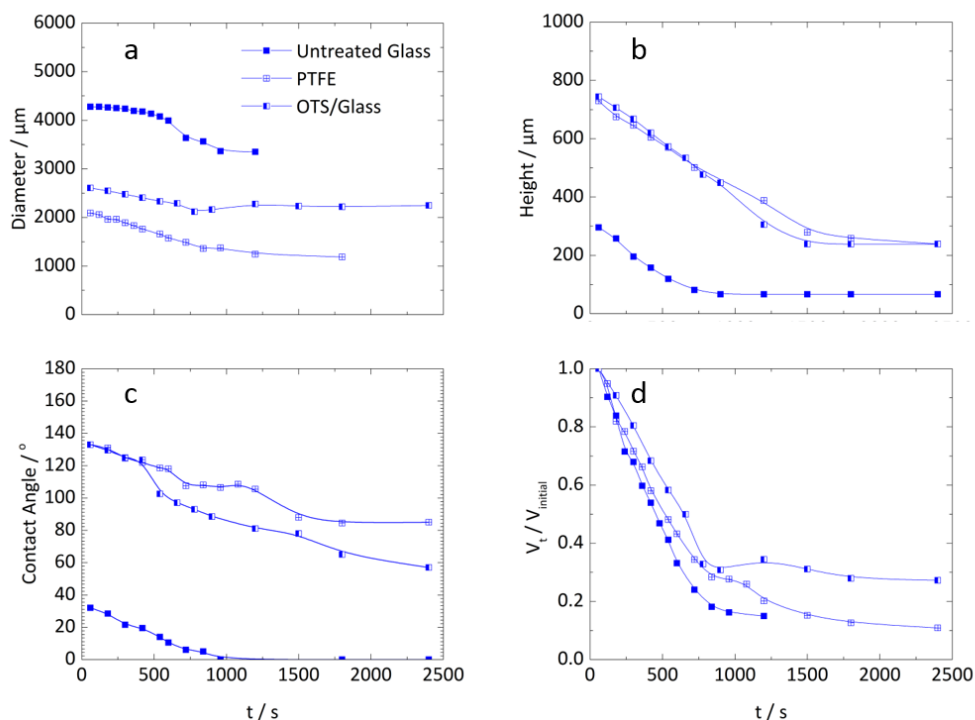


Figure S9: Corresponding variation in diameter (a), height (b), contact angle (c) and reduced volume (d) with time for the extractions on different substrates imaged in Figure S7. Images were thresholded and pixel intensity was processed to extract diameter and height and calculated volume. Contact angle was measured manually and averaged across both sides of the planar image. In all cases, the dependent variable decreased monotonically up to a point, normally denoted in previous analysis as τ , before remaining constant with time. Lines are added to guide the eye.

References

- [1] J. B. Lewis, Journal of Applied Chemistry, 1955, 5, 228-237).
- [2] T. Watanabe, C. G. Lopez, J. F. Douglas, T. Ono, J. T. Cabral, " Microfluidic Approach for the Formation of Internally Porous Polymer Particles by Solvent Extraction" Langmuir 30, 2470-2479 (2014)
- [3] C. E. Udoh, V. Garbin, and J.T. Cabral, "Microporous polymer particles via phase inversion in microfluidics: impact of non-solvent quality" Langmuir 32 (32), pp 8131–8140 (2016)
- [4] C. E. Udoh, J. T. Cabral, and V. Garbin "Nanocomposite capsules with directional, pulsed nanoparticle release" Science Advances, 3, 12, eaao3353 (2017)